

C–H Activation

International Edition: DOI: 10.1002/anie.201909457
 German Edition: DOI: 10.1002/ange.201909457

Arene-Free Ruthenium(II/IV)-Catalyzed Bifurcated Arylation for Oxidative C–H/C–H Functionalizations

Torben Rogge and Lutz Ackermann*

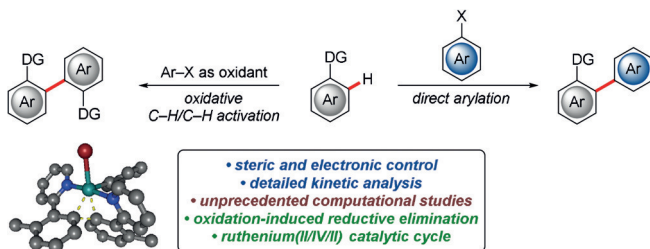
Abstract: Experimental and computational studies provide detailed insight into the selectivity- and reactivity-controlling factors in bifurcated ruthenium-catalyzed direct C–H arylations and dehydrogenative C–H/C–H functionalizations. Thorough investigations revealed the importance of arene-ligand-free complexes for the formation of biscyclometalated intermediates within a ruthenium(II/IV/II) mechanistic manifold.

Over the last decade, catalyzed C–H activation has gained considerable momentum and has emerged as a powerful tool in molecular synthesis^[1] with applications in the pharmaceutical industry,^[2] materials science,^[3] and for the synthesis of agrochemicals.^[4] Among the commonly used transition-metal catalysts, ruthenium^[5] offers an effective, economically attractive alternative to more costly palladium, platinum, or iridium catalysts,^[6] often proceeding through mechanistically distinct pathways. Thus, protocols for the direct C–H arylation under ruthenium catalysis have been developed,^[7] with major contributions by Oi/Inoue,^[8] Dixneuf,^[9] and our group,^[10] among others.^[11] Despite the wealth of viable canonical, isohypsic arylations, studies on more challenging ruthenium-catalyzed dehydrogenative C–H/C–H activation for the formation of C–C bonds continue to be largely limited to the use of costly metal salts as terminal oxidants.^[12] In contrast, exploiting the potential of mild aryl halides as oxidants through a unique manifold has been significantly hampered by scarce mechanistic insights.^[13] Within our studies on ruthenium-catalyzed C–H activation,^[14] we obtained key insights into the working mode of bifurcated C–H arylations and oxidative C–H/C–H activations, on which we report herein. Notable results of this study comprise (Scheme 1):

- 1) Chemoselectivity control through the judicious choice of stereoelectronic properties.
- 2) Decoordination of *p*-cymene for the in situ formation of an arene-ligand-free active catalyst.
- 3) Detailed mechanistic insights by DFT calculations,^[15] providing strong support for a turnover-limiting oxidative addition event.

[*] T. Rogge, Prof. Dr. L. Ackermann
 Institut für Organische und Biomolekulare Chemie
 Georg-August-Universität Göttingen
 Tammannstraße 2, 37077 Göttingen (Germany)
 E-mail: Lutz.Ackermann@chemie.uni-goettingen.de
 Homepage: <http://www.ackermann.chemie.uni-goettingen.de>

Supporting information and the ORCID identification number(s) for the author(s) of this article can be found under:
<https://doi.org/10.1002/anie.201909457>.



Scheme 1. Bifurcated ruthenium(II/IV)-catalyzed C–H/C–H arylations. Bottom left: Structure of key transition state.

- 4) An energetically favorable ruthenium(II/IV/II) catalytic manifold.

We initiated our studies by probing the effect exerted by various aryl halides **2** in the carboxylate-assisted C–H activation of arene **1** (Figure 1). Aryl halide **2e** devoid of a substituent in the *ortho*-position and 2-fluoro-substituted **2f** furnished the expected arylated products **3** in excellent yield and selectivity. In sharp contrast, aryl halides **2h–m**, which bear an electron-withdrawing substituent in the 2-position, led to bifurcation in terms of a preferential formation of the C–H/C–H activation product **4**. Aryl chlorides were found to be less reactive, while bromides and iodides showed com-

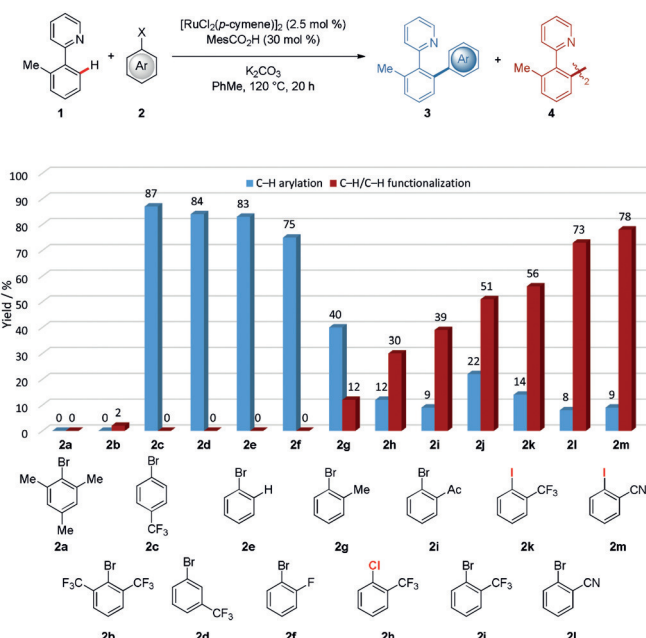


Figure 1. Bifurcated C–H arylations with halides **2**. Yields of isolated products are given. Mes = 2,4,6-trimethylphenyl.

parable reactivities, with sterically congested 2,6-disubstitution being less well tolerated.

Variation of the arylpyridine **1** revealed a strong influence of its substitution pattern on the bifurcated course of the reaction (Figure 2). Thus, substrates devoid of *ortho*-substituents and heteroatom-substituted compounds **1b** and **1d** exclusively furnished the C–H arylated products **3**, while substrates **1a** and **1g,h** containing alkyl or benzyl groups in the 2-position underwent the oxidative C–H/C–H activation process with high levels of selectivity.

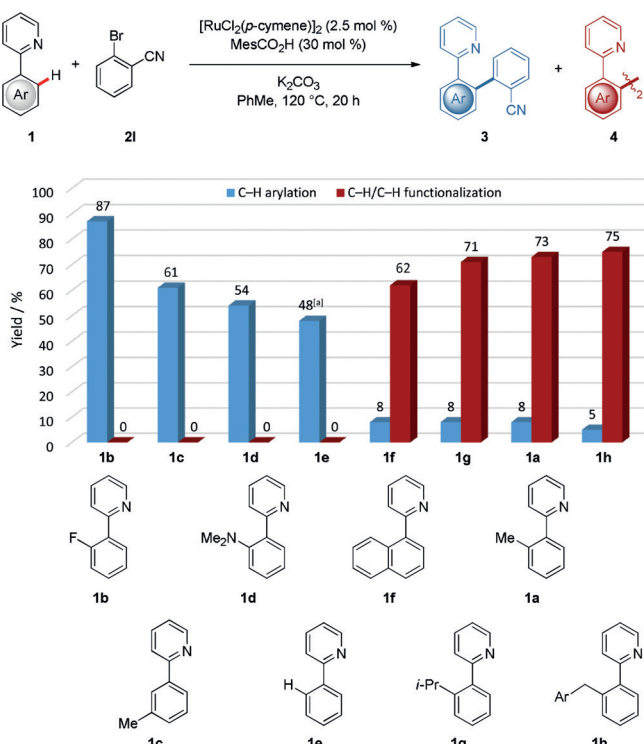


Figure 2. Influence of the phenylpyridine substitution pattern. Yield of isolated products are given. [a] Bis-arylated product was obtained.

Ar = 4-F-C₆H₄.

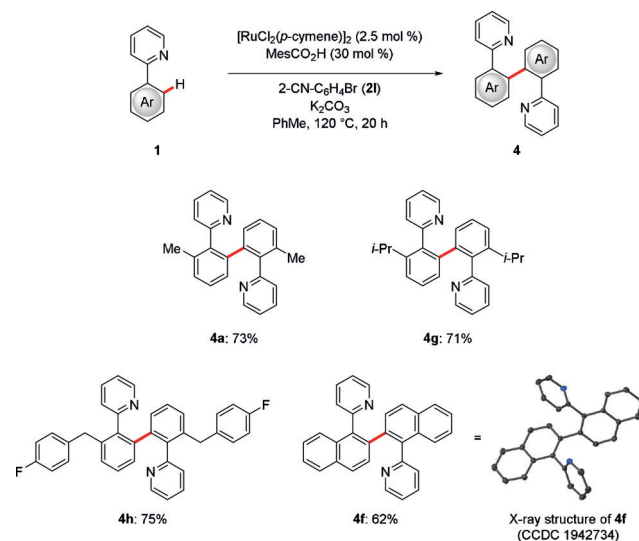
Subsequently, the influence of the reaction medium on the chemoselectivity was studied. The use of apolar solvents as the reaction medium resulted in a mixture of products with comparable performances (Table 1, entries 1–5). Interestingly, when polar, aprotic MeCN was employed as the solvent, product **4a** was obtained as the sole product in high yield (entry 6), while other polar solvents fell short in providing comparable efficacies (entries 7–9). Furthermore, the essential roles of the ruthenium catalyst and the MesCO₂H additive were confirmed (entries 2 and 3), substantiating the importance of carboxylate assistance.^[16] A cyclometalated complex failed to provide improved results (entry 11).

The developed C–H/C–H activation strategy allowed the rapid construction of densely substituted biaryls in good yields and excellent levels of regioselectivity (Scheme 2). It is noteworthy that compound **1f** containing a valuable naphthyl

Table 1: Influence of the reaction medium.^[a]

Entry	Deviation from the standard conditions	3a [%]	4a [%]
1	–	22	51
2	without [Ru]	–	–
3	without MesCO ₂ H	8 ^[b]	8 ^[b]
4	[Ru(O ₂ CMes) ₂ (<i>p</i> -cymene)] (5.0 mol %), without MesCO ₂ H	24	57
5	dioxane as solvent	25	40
6	MeCN as solvent	trace	78
7	NMP as solvent	13	18
8	DMSO as solvent	–	–
9	DMF as solvent	11 ^[b]	18 ^[b]
10	<i>p</i> -cymene (1.0 equiv) added	22	54
11	(5.0 mol %)	22	55

[a] Reaction conditions: **1a** (0.50 mmol), **2I** (0.75 mmol), [RuCl₂(*p*-cymene)]₂ (2.5 mol %), MesCO₂H (30 mol %), PhMe (2.0 mL), 120 °C, 20 h. Yields of isolated products are given. [b] Conversion determined by ¹H NMR analysis using 4-(MeO₂C)₂C₆H₄ as the internal standard.

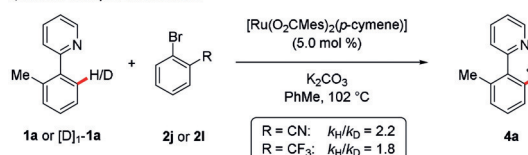


Scheme 2. Ruthenium-catalyzed dehydrogenative C–H/C–H arylation.

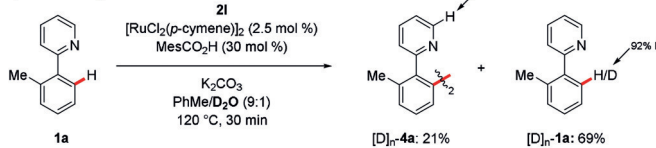
moiety efficiently underwent the desired transformation, delivering 2,2'-binaphthyl **4f** in high yield.^[17]

Intrigued by the bifurcation behavior of the ruthenium-catalyzed C–H arylation manifold, we became interested in unraveling the catalyst's mode of action. Kinetic isotope effect (KIE) studies with the two best performing aryl bromides revealed KIE values of $k_H/k_D \approx 2.2$ and 1.8, respectively (Scheme 3a). A reaction in the presence of isotopically labeled D₂O as the cosolvent led to significant H/D scrambling in the *ortho*-position of recovered substrate **1a**, indicating a reversible C–H cleavage (Scheme 3b). Careful analysis of the reaction mixture resulted in the detection of

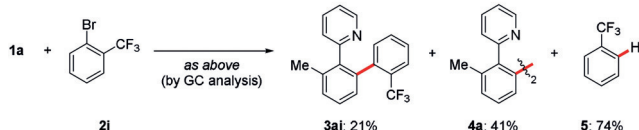
a) Kinetic Isotope Effect Studies



b) H/D Exchange



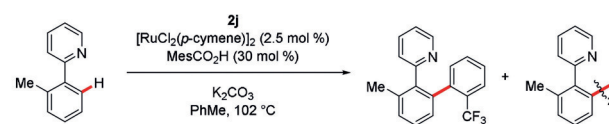
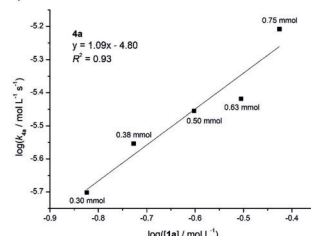
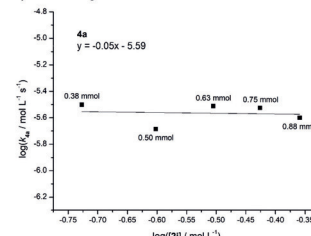
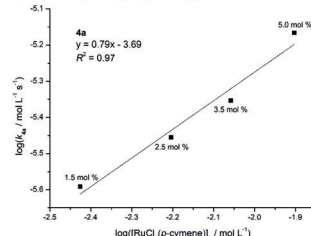
c) Detection of Byproducts

**Scheme 3.** Key mechanistic findings.

74% of PhCF_3 as byproduct, confirming aryl bromide **2** as the terminal oxidant (Scheme 3c).

Furthermore, during the course of the reaction, a substantial amount of *p*-cymene decoordination from the ruthenium precatalyst was observed. Hence, after a reaction time of 3 min, 26% of free *p*-cymene was detected, with this amount further increasing to more than 70%. These findings are indicative of an arene-ligand-free complex being catalytically competent (Figure 3).^[18] Similar results were obtained irrespective of the nature of the employed substrates **1** and **2** (Figures S4–S6 in the Supporting Information).

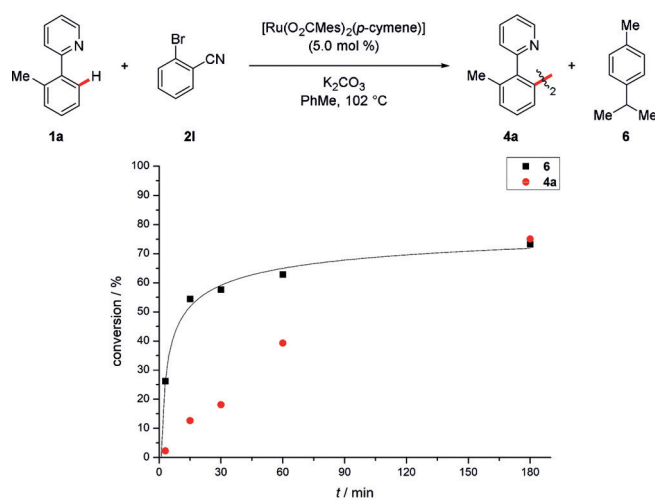
Detailed kinetic analysis revealed a reaction order of 1 with respect to the phenylpyridine concentration for the C–H/C–H activation as well as for the C–H arylation process (Figures 4a and S7). No dependence on the aryl halide concentration was observed (Figure 4b), while a positive

a) Order in **1a**b) Order in **2j**c) Order in $[\text{RuCl}_2(\text{p-cymene})]_2$ **Figure 4.** Kinetic analysis.

reaction order was found with respect to the catalyst concentration (Figure 4c).^[19]

Motivated by our findings we became interested in further investigating the reaction mechanism by means of density functional theory (DFT) calculations at the PBE0-D3(BJ)/def2-TZVP + SMD(MeCN)//TPSS-D3(BJ)/def2-TZVP level of theory.^[20] C–H ruthenation on one out of two coordinated arylpyridine motifs occurs through formation of agostic complex **B**, generating ruthenacyclic intermediate **C** (Figure 5). Then, C–H ruthenation on the second substrate leads to the generation of the biscyclometalated complex **E**, which was calculated to be $-0.6 \text{ kcal mol}^{-1}$ more stable than adduct **A**. In the presence of a nitrile either as solvent or reagent, ligand exchange can occur on intermediate **C**, which stabilizes the complex and reduces the energy barrier for the second C–H ruthenation process. Subsequently, a turnover-limiting oxidative addition of the aryl halide forms ruthenium(IV) intermediate **H**, providing support for an oxidation-induced reductive elimination event.^[21] Employing 2-bromobenzonitrile as the oxidant further reduces the energy of the oxidative addition elementary step by $3.8 \text{ kcal mol}^{-1}$ (Figure S10). It is also noteworthy that a ruthenium(II/0/II) manifold as well as higher spin states were shown to be unlikely to be operative (Figure S11 and Table S13).

The oxidative addition of the parent bromobenzene **2e** facilitates the reductive elimination between the aryl ligands, leading to the preferential formation of the arylated compound **3ae**. In sharp contrast, the use of 2-bromobenzonitrile (**2l**) as the aryl halide led to a distinct change in the chemoselectivity, favoring formation of the C–H/C–H activated product **4a** with $\Delta\Delta G^{\ddagger}_{\text{TS6-TS7}}$ values of $3.9 \text{ kcal mol}^{-1}$

**Figure 3.** Detection of free *p*-cymene.

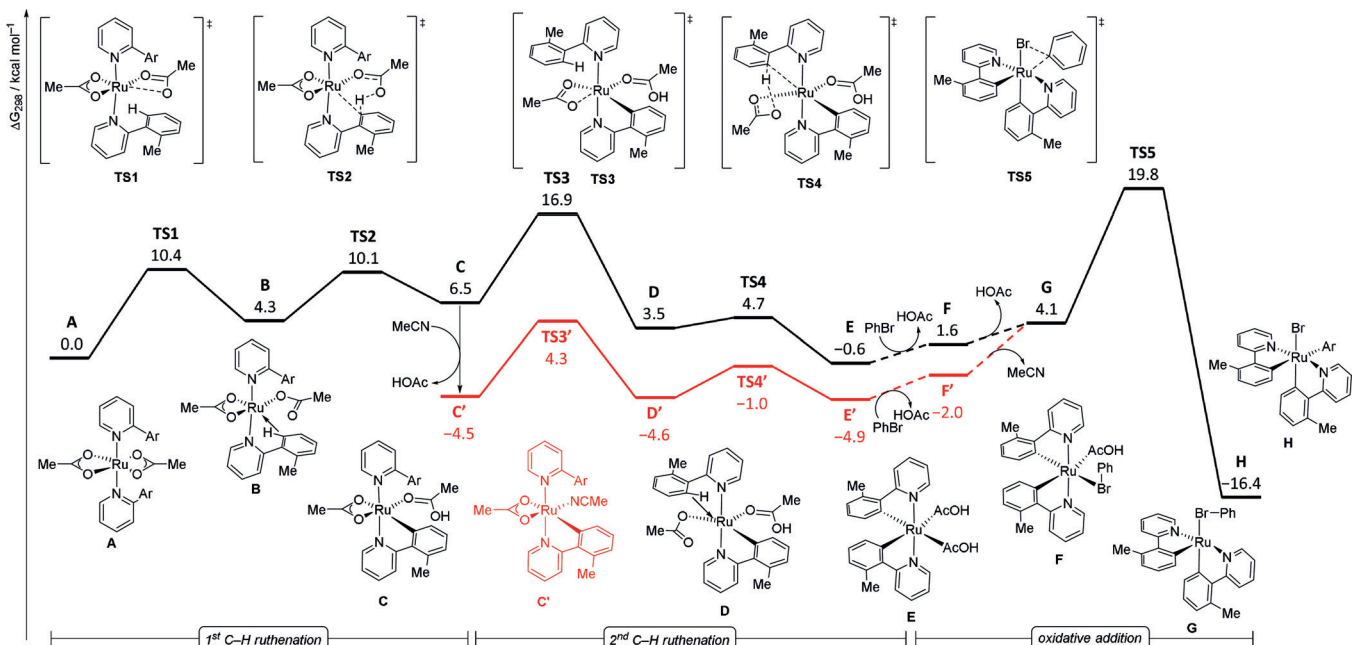


Figure 5. Gibbs free energy diagram for the formation of biscyclometalated complex **E** and oxidative addition at the PBE0-D3(BJ)/def2-TZVP + SMD(MeCN)//TPSS-D3(BJ)/def2-TZVP level of theory. Ar = *o*-tolyl.

and $-5.7 \text{ kcal mol}^{-1}$, respectively, for bromobenzene and 2-bromobenzonitrile, with the aryl moiety acting as an electron-withdrawing spectator ligand (Figure 6).^[22] Thereafter, protodemetalation liberates the desired product and regenerates the catalytically active complexes **A** and **C**, respectively (Schemes S1–S3).

A detailed bond order analysis of the relevant C–H ruthenation steps within a More O’Ferrall–Jencks plot is suggestive of a base-assisted internal electrophilic substitution (BIES)^[23] rather than a conventional concerted metalation/deprotonation (CMD)^[24] C–H cleavage event (Figures 7 and S12).^[20]

In conclusion, we have reported on detailed insight into bifurcated ruthenium-catalyzed oxidative C–H/C–H activations. Combined experimental and theoretical mechanistic studies revealed the bifurcated C–H arylation manifold

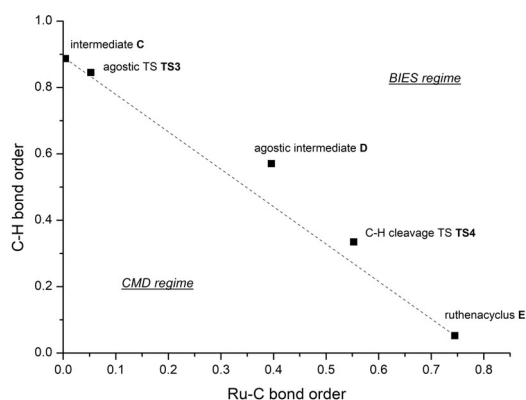


Figure 7. More O’Ferrall–Jencks plot for the C–H ruthenation step.

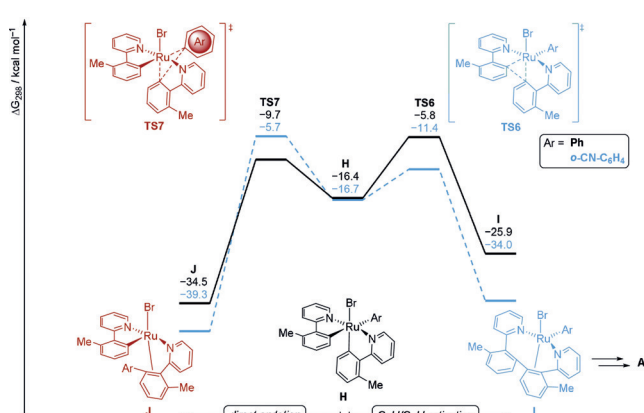


Figure 6. Gibbs free energy diagram for the selectivity-determining reductive elimination for the bifurcated C–H arylation.

through an arene-ligand-free ruthenium complex as the catalytically competent species. In this context, comprehensive DFT computations provided strong support for the formation of a biscyclometalated complex as well as an oxidation-induced reductive elimination process within a ruthenium(II/IV/II) manifold.

Acknowledgements

Generous support by the DFG (SPP1807 and Gottfried-Wilhelm-Leibniz award to L.A.) is gratefully acknowledged.

Conflict of interest

The authors declare no conflict of interest.

Keywords: C–H activation · density functional calculations · oxidative catalysis · reaction mechanisms · ruthenium

How to cite: *Angew. Chem. Int. Ed.* **2019**, *58*, 15640–15645
Angew. Chem. **2019**, *131*, 15787–15792

- [1] For recent reviews, see: a) S. M. Khake, N. Chatani, *Trends Chem.* **2019**, *1*, 524–539; b) P. Gandeepan, T. Müller, D. Zell, G. Cera, S. Warratz, L. Ackermann, *Chem. Rev.* **2019**, *119*, 2192–2452; c) P. H. Dixneuf, J. F. Soule, *Chem. Rev.* **2018**, *118*, 7532–7585; d) P. Gandeepan, L. Ackermann, *Chem.* **2018**, *4*, 199–222; e) C. S. Wang, J. C. K. Chu, T. Rovis, *Angew. Chem. Int. Ed.* **2018**, *57*, 62–101; *Angew. Chem.* **2018**, *130*, 64–105; f) K. Murakami, S. Yamada, T. Kaneda, K. Itami, *Chem. Rev.* **2017**, *117*, 9302–9332; g) Y. Park, Y. Kim, S. Chang, *Chem. Rev.* **2017**, *117*, 9247–9301; h) J. He, M. Wasa, K. S. L. Chan, Q. Shao, J.-Q. Yu, *Chem. Rev.* **2017**, *117*, 8754–8786; i) J. F. Hartwig, M. A. Larsen, *ACS Cent. Sci.* **2016**, *2*, 281–292; j) L. McMurray, F. O’Hara, M. J. Gaunt, *Chem. Soc. Rev.* **2011**, *40*, 1885–1898, and references therein.
- [2] a) T. Cernak, K. D. Dykstra, S. Tyagarajan, P. Vachal, S. W. Krska, *Chem. Soc. Rev.* **2016**, *45*, 546–576; b) M. Seki, *Org. Process Res. Dev.* **2016**, *20*, 867–877; c) L. Ackermann, *Org. Process Res. Dev.* **2015**, *19*, 260–269.
- [3] a) T. Bura, J. T. Blaskovits, M. Leclerc, *J. Am. Chem. Soc.* **2016**, *138*, 10056–10071; b) D. J. Schipper, K. Fagnou, *Chem. Mater.* **2011**, *23*, 1594–1600.
- [4] J. Hubrich, T. Himmler, L. Rodefeld, L. Ackermann, *ACS Catal.* **2015**, *5*, 4089–4093.
- [5] For selected reviews, see: a) P. Nareddy, F. Jordan, M. Szostak, *ACS Catal.* **2017**, *7*, 5721–5745; b) J. A. Leitch, C. G. Frost, *Chem. Soc. Rev.* **2017**, *46*, 7145–7153; c) C. Bruneau, P. H. Dixneuf, *Top. Organomet. Chem.* **2015**, *55*, 137–188; d) C. Bruneau, *Top. Organomet. Chem.* **2014**, *48*, 195–236; e) P. B. Arockiam, C. Bruneau, P. H. Dixneuf, *Chem. Rev.* **2012**, *112*, 5879–5918; f) N. Chatani, S. Inoue, K. Yokota, H. Tatamidani, Y. Fukumoto, *Pure Appl. Chem.* **2010**, *82*, 1443–1451; g) L. Ackermann, R. Vicente, *Top. Curr. Chem.* **2010**, *292*, 211–229; h) L. Ackermann, R. Vicente, A. R. Kapdi, *Angew. Chem. Int. Ed.* **2009**, *48*, 9792–9826; *Angew. Chem.* **2009**, *121*, 9976–10011.
- [6] On July 1, 2019, the prices of platinum, rhodium, iridium, palladium, and ruthenium were 837, 3350, 1480, 1549, and 253 US\$ per troy oz, respectively. See: <http://www.platinum.matthey.com/prices/price-charts>.
- [7] B. Li, P. H. Dixneuf, *Chem. Soc. Rev.* **2013**, *42*, 5744–5767.
- [8] a) S. Oi, E. Aizawa, Y. Ogino, Y. Inoue, *J. Org. Chem.* **2005**, *70*, 3113–3119; b) S. Oi, S. Fukita, N. Hirata, N. Watanuki, S. Miyano, Y. Inoue, *Org. Lett.* **2001**, *3*, 2579–2581.
- [9] a) B. Li, C. Darcel, P. H. Dixneuf, *ChemCatChem* **2014**, *6*, 127–130; b) B. Li, C. B. Bheeter, C. Darcel, P. Dixneuf, *Top. Catal.* **2014**, *57*, 833–842; c) K. S. Singh, P. H. Dixneuf, *ChemCatChem* **2013**, *5*, 1313–1316; d) E. Ferret Flegeau, C. Bruneau, P. H. Dixneuf, A. Jutand, *J. Am. Chem. Soc.* **2011**, *133*, 10161–10170; e) B. Li, C. B. Bheeter, C. Darcel, P. H. Dixneuf, *ACS Catal.* **2011**, *1*, 1221–1224; f) P. B. Arockiam, C. Fischmeister, C. Bruneau, P. H. Dixneuf, *Angew. Chem. Int. Ed.* **2010**, *49*, 6629–6632; *Angew. Chem.* **2010**, *122*, 6779–6782; g) I. Özdemir, S. Demir, B. Çetinkaya, C. Gourlaouen, F. Maseras, C. Bruneau, P. H. Dixneuf, *J. Am. Chem. Soc.* **2008**, *130*, 1156–1157.
- [10] a) S. R. Yetra, T. Rogge, S. Warratz, J. Struwe, W. Peng, P. Vana, L. Ackermann, *Angew. Chem. Int. Ed.* **2019**, *58*, 7490–7494; *Angew. Chem.* **2019**, *131*, 7569–7573; b) R. Mei, C. Zhu, L. Ackermann, *Chem. Commun.* **2016**, *52*, 13171–13174; c) L. Ackermann, A. V. Lygin, *Org. Lett.* **2011**, *13*, 3332–3335; d) L. Ackermann, R. Vicente, H. K. Potukuchi, V. Pirovano, *Org. Lett.* **2010**, *12*, 5032–5035; e) L. Ackermann, R. Born, P. Alvarez-Bercedo, *Angew. Chem. Int. Ed.* **2007**, *46*, 6364–6367; *Angew. Chem.* **2007**, *119*, 6482–6485; f) L. Ackermann, A. Althammer, R. Born, *Angew. Chem. Int. Ed.* **2006**, *45*, 2619–2622; *Angew. Chem.* **2006**, *118*, 2681–2685; g) L. Ackermann, *Org. Lett.* **2005**, *7*, 3123–3125.
- [11] a) Y. Koseki, K. Kitazawa, M. Miyake, T. Kochi, F. Kakiuchi, *J. Org. Chem.* **2017**, *82*, 6503–6510; b) C. J. Teskey, S. M. A. Sohel, D. L. Bunting, S. G. Modha, M. F. Greaney, *Angew. Chem. Int. Ed.* **2017**, *56*, 5263–5266; *Angew. Chem.* **2017**, *129*, 5347–5350; c) A. Biafora, T. Krause, D. Hackenberger, F. Belitz, L. J. Gooßen, *Angew. Chem. Int. Ed.* **2016**, *55*, 14752–14755; *Angew. Chem.* **2016**, *128*, 14972–14975; d) L. Huang, D. J. Weix, *Org. Lett.* **2016**, *18*, 5432–5435; e) R. K. Chinnagolla, M. Jegannathan, *Chem. Commun.* **2014**, *50*, 2442–2444; f) Y. Aihara, N. Chatani, *Chem. Sci.* **2013**, *4*, 664–670; g) N. Dastbaravardeh, M. Schnürch, M. D. Mihovilovic, *Org. Lett.* **2012**, *14*, 1930–1933; h) F. Kakiuchi, S. Kan, K. Igi, N. Chatani, S. Murai, *J. Am. Chem. Soc.* **2003**, *125*, 1698–1699.
- [12] For a review, see: a) C.-J. Li, *Acc. Chem. Res.* **2009**, *42*, 335–344; for selected examples, see: b) S. Dana, D. Chowdhury, A. Mandal, F. A. S. Chipem, M. Baidya, *ACS Catal.* **2018**, *8*, 10173–10179; c) D. Srimani, Y. Ben-David, D. Milstein, *Angew. Chem. Int. Ed.* **2013**, *52*, 4012–4015; *Angew. Chem.* **2013**, *125*, 4104–4107; d) J. Dong, Z. Long, F. Song, N. Wu, Q. Guo, J. Lan, J. You, *Angew. Chem. Int. Ed.* **2013**, *52*, 580–584; *Angew. Chem.* **2013**, *125*, 608–612; e) X. Guo, G. Deng, C.-J. Li, *Adv. Synth. Catal.* **2009**, *351*, 2071–2074; f) S. Oi, H. Sato, S. Sugawara, Y. Inoue, *Org. Lett.* **2008**, *10*, 1823–1826; g) G. Deng, L. Zhao, C.-J. Li, *Angew. Chem. Int. Ed.* **2008**, *47*, 6278–6282; *Angew. Chem.* **2008**, *120*, 6374–6378.
- [13] L. Ackermann, P. Novák, R. Vicente, V. Pirovano, H. K. Potukuchi, *Synthesis* **2010**, 2245–2253.
- [14] L. Ackermann, *Acc. Chem. Res.* **2014**, *47*, 281–295.
- [15] a) D. L. Davies, S. A. Macgregor, C. L. McMullin, *Chem. Rev.* **2017**, *117*, 8649–8709; b) D. Balcells, E. Clot, O. Eisenstein, *Chem. Rev.* **2010**, *110*, 749–823.
- [16] L. Ackermann, *Chem. Rev.* **2011**, *111*, 1315–1345.
- [17] CCDC 1942734 contains the supplementary crystallographic data for this paper. These data can be obtained free of charge from The Cambridge Crystallographic Data Centre.
- [18] a) M. Simonetti, D. M. Cannas, X. Just-Baringo, I. J. Vitorica-Yrezabal, I. Larrosa, *Nat. Chem.* **2018**, *10*, 724–731; b) J. McIntyre, I. Mayoral-Soler, P. Salvador, A. Poater, D. J. Nelson, *Catal. Sci. Technol.* **2018**, *8*, 3174–3182; c) M. Simonetti, G. J. Perry, X. C. Cambeiro, F. Julia-Hernandez, J. N. Arokianathan, I. Larrosa, *J. Am. Chem. Soc.* **2016**, *138*, 3596–3606; d) P. Marcé, A. J. Paterson, M. F. Mahon, C. G. Frost, *Catal. Sci. Technol.* **2016**, *6*, 7068–7076; e) H. H. Al Mamari, E. Diers, L. Ackermann, *Chem. Eur. J.* **2014**, *20*, 9739–9743; f) L. Ackermann, A. Althammer, R. Born, *Tetrahedron* **2008**, *64*, 6115–6124; g) L. Ackermann, A. Althammer, R. Born, *Synlett* **2007**, 2833–2836.
- [19] It is noteworthy that a complex kinetic behavior was observed when 2-bromobenzonitrile was employed as a reagent, indicating a distinct change in mechanism (Figure S9).
- [20] For details, see the Supporting Information.
- [21] a) J. Kim, K. Shin, S. Jin, D. Kim, S. Chang, *J. Am. Chem. Soc.* **2019**, *141*, 4137–4146; b) S. Y. Hong, Y. Park, Y. Hwang, Y. B. Kim, M.-H. Baik, S. Chang, *Science* **2018**, *359*, 1016–1021; c) K. Shin, Y. Park, M.-H. Baik, S. Chang, *Nat. Chem.* **2017**, *10*, 218–224.
- [22] E. Zuidema, P. W. N. M. van Leeuwen, C. Bo, *Organometallics* **2005**, *24*, 3703–3710.

- [23] a) K. Naksomboon, J. Poater, F. M. Bickelhaupt, M. Á. Fernández-Ibáñez, *J. Am. Chem. Soc.* **2019**, *141*, 6719–6725; b) D. Zell, M. Bursch, V. Müller, S. Grimme, L. Ackermann, *Angew. Chem. Int. Ed.* **2017**, *56*, 10378–10382; *Angew. Chem.* **2017**, *129*, 10514–10518; c) W. Ma, R. Mei, G. Tenti, L. Ackermann, *Chem. Eur. J.* **2014**, *20*, 15248–15251.
- [24] S. I. Gorelsky, D. Lapointe, K. Fagnou, *J. Am. Chem. Soc.* **2008**, *130*, 10848–10849.

Manuscript received: July 27, 2019

Revised manuscript received: August 20, 2019

Accepted manuscript online: September 2, 2019

Version of record online: September 20, 2019
